

Systematic Comparison of Tsallis Statistics for Charged Pions Produced In pp Collisions

A.S. Parvan^{1,2}, O.V. Teryaev¹, and J. Cleymans³

¹ Bogoliubov Laboratory of Theoretical Physics, Joint Institute for Nuclear Research, Dubna, Russian Federation

² Department of Theoretical Physics, Horia Hulubei National Institute of Physics and Nuclear Engineering, Bucharest-Magurele, Romania

³ UCT-CERN Research Centre and Department of Physics, University of Cape Town, South Africa

Received: date / Revised version: date

Abstract. The energy dependence of Tsallis statistics parameters is presented for charged pions produced at beam energies ranging between 6.3 GeV and 7 TeV. It is found that deviations from Boltzmann statistics are monotonically growing with beam energy. The energy dependence of the parameters T and q of the negatively charged pions in the energy range $6.3 < \sqrt{s} < 7000$ GeV reveals that the deviation of the transverse momentum distribution from the exponential becomes more and more pronounced as the beam energy is increased. The parameter q increases with beam energy while the temperature T slowly decreases.

PACS. 13.85.-t Hadron-induced high- and super-high-energy interactions – 13.85.Hd Inelastic scattering: many-particle final states – 24.60.-k Statistical theory and fluctuations

1 Introduction

The use of non-extensive distributions (commonly referred to as Tsallis distributions [1]) in high-energy physics has a long history [2, 3, 4, 5, 6, 7, 8, 9, 10]. They have been surprisingly successful in describing transverse momentum distributions in p-p collisions at the LHC. At first these were used as a parametrization of the experimental data [11, 12, 13, 14, 15, 16, 17, 18, 19, 20, 21] and, more recently, they have attracted considerable attention in theoretical papers [22, 23, 24, 25, 26, 27, 28, 29, 30, 31]. The parametrization holds extremely well even in the high transverse momentum region traditionally reserved for perturbative QCD as shown in [32, 33, 34, 35, 36]. This is indeed unexpected and should be viewed with some skepticism, it definitely calls for further investigations.

In the present paper we extend the analysis to lower beam energies and include results from the NA61 collaboration [37] for negatively charged pions measured at $p_{\text{lab}} = 20, 31, 40, 80$ and 158 GeV/c, as well as results from the STAR [11, 12], PHENIX [13, 14], ALICE [15, 16], ATLAS [21] and CMS [18, 19, 20] collaborations.

The energy dependence of the parameters T and q of the negatively charged pions in the energy range $6.3 < \sqrt{s} < 7000$ GeV reveals that the deviation of the transverse momentum distribution from the exponential becomes more and more pronounced as the beam energy is increased. The parameter q increases with beam energy while the temperature T slowly decreases.

2 Transverse momentum distributions in pp collisions

The experimental results on the transverse momentum distributions for negatively charged pions are fitted to the Tsallis distribution as used in Ref. [30]. The explicit form used is given by the following expression

$$\frac{d^2 N}{dp_T dy} = gV \frac{p_T m_T \cosh y}{(2\pi)^2} \times \left[1 + (q-1) \frac{m_T \cosh y - \mu}{T} \right]^{q/(1-q)}, \quad (1)$$

where $m_T = \sqrt{p_T^2 + m^2}$, m is the particle rest mass, μ, T, V are the chemical potential, temperature, and volume, g is the spin degeneracy factor and q is a parameter whose range will be discussed in detail below. In the limit where the parameter $q \rightarrow 1$ one recovers the Maxwell-Boltzmann distribution:

$$\frac{d^2 N}{dp_T dy} = gV \frac{p_T m_T \cosh y}{(2\pi)^2} e^{-\frac{m_T \cosh y - \mu}{T}}. \quad (2)$$

Obviously the integral of Eq. (1) over all transverse momenta and rapidities has to exist in order to produce a finite number of particles, this leads to the constraint that $q < 3/2$. For massless particles the integral can be calculated analytically, the zero chemical potential case is given by:

$$n = \frac{g T^3}{\pi^2} \frac{1}{(2-q)(3-2q)}. \quad (3)$$

While the energy density is given by:

$$\epsilon = \frac{g}{\pi^2} \frac{3T^4}{(2-q)(3-2q)(4-3q)}. \quad (4)$$

which leads to a more stringent condition

$$q < \frac{4}{3}. \quad (5)$$

In contrast to the exact Tsallis statistics [1], the single-particle distribution function (1) of the Tsallis-factorized statistics is represented in a simple explicit form and serves as a powerful tool to study the experimental data on the transverse momentum distributions. The single-particle distribution function of the Tsallis statistics cannot be written in an explicit form (1) because the many-body distribution function of the exact Tsallis statistics does not factorize into the product of the single-particle distribution functions [38]. Only in the factorization (dilute gas) approximation the single-particle distribution functions of the Tsallis statistics can be written explicitly [39]. For simplicity we will refer to Eq. 1 as Tsallis distribution.

For a given rapidity range $y_0 < y < y_1$ the transverse momentum distribution can be written as

$$\left. \frac{d^2N}{dp_T dy} \right|_{y_0 < y < y_1} = gV \frac{p_T m_T}{(2\pi)^2} \int_{y_0}^{y_1} dy \cosh y \times \left[1 + (q-1) \frac{m_T \cosh y - \mu}{T} \right]^{q/(1-q)}. \quad (6)$$

At mid-rapidity $y = 0$ and chemical potential $\mu = 0$ the distribution function (1) reduces to

$$\frac{d^2N}{dp_T dy} = gV \frac{p_T m_T}{(2\pi)^2} \left[1 + (q-1) \frac{m_T}{T} \right]^{q/(1-q)}. \quad (7)$$

Let us study the changes in the transverse momentum distribution of the negatively charged pions π^- (selected just because the data are available at all the considered energies) are produced in pp collisions with energy in the range from $\sqrt{s} = 6.3$ GeV to 7000 GeV. Figure 1 represents the transverse momentum distribution of π^- pions produced in the pp collisions as obtained by the NA61/SHINE Collaboration [37] at $\sqrt{s} = 6.3, 7.7, 8.8, 12.3$ and 17.3 GeV (which are close to the energy range of the future NICA collider) in the rapidity interval $0 < y < 0.2$. The symbols represent the experimental data. The solid curves are the fits to the experimental data using the Tsallis function (6). The values of the parameters are given in Table 1. The Tsallis function describes very well the experimental data. At the energies of the NA61/SHINE Collaboration the transverse momentum distribution of negatively charged pions π^- has the power law form, however, its deviation from the exponential function is not so large. The values of the parameter q are close to unity. Herewith, the temperature T is approximately $T \sim 100$ MeV. Moreover, the value of the radius R is large in comparison to the geometrical sizes of the system composed

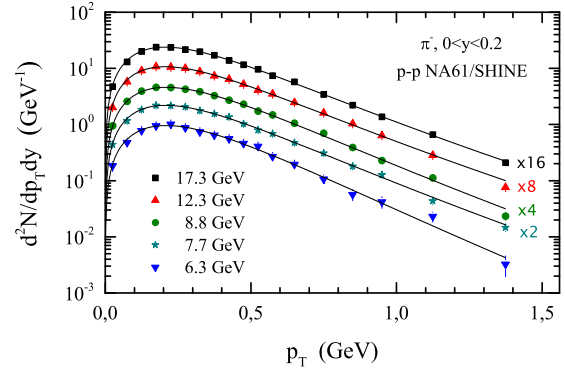


Fig. 1. (Color online) Transverse momentum distribution of negatively charged pions π^- produced in pp collisions as obtained by the NA61/SHINE Collaboration [37] at $\sqrt{s} = 6.3, 7.7, 8.8, 12.3$ and 17.3 GeV in the rapidity interval $0 < y < 0.2$. The solid curves are the fits of the data to the Tsallis distribution (6).

from two protons. Note that the experimental data of the NA61/SHINE Collaboration were also fitted to the Tsallis function in Ref. [31], we can reproduce these results within the limits of errors at $y = 0$.

Figure 2 presents the transverse momentum distributions of π^- pions produced in the proton-proton collisions as obtained by the PHENIX Collaboration [13,14] at $\sqrt{s} = 200$ and 62.4 GeV at mid-rapidity and by the STAR Collaboration [11,12] at $\sqrt{s} = 200$ GeV. The symbols represent the experimental data of the PHENIX and STAR Collaborations. The solid curves are the fits of the experimental data to the Tsallis function (7) divided by the geometrical factor $2\pi p_T$:

$$\frac{1}{2\pi p_T} \frac{d^2N}{dp_T dy} = gV \frac{m_T}{(2\pi)^3} \left[1 + (q-1) \frac{m_T}{T} \right]^{q/(1-q)}. \quad (8)$$

The values of the parameters of this Tsallis function are given in Table 1. The experimental data for the transverse momentum distributions of the negatively charged pions π^- are very well described by the function (8). The experimental transverse momentum distributions of π^- pions measured by the PHENIX and STAR Collaborations

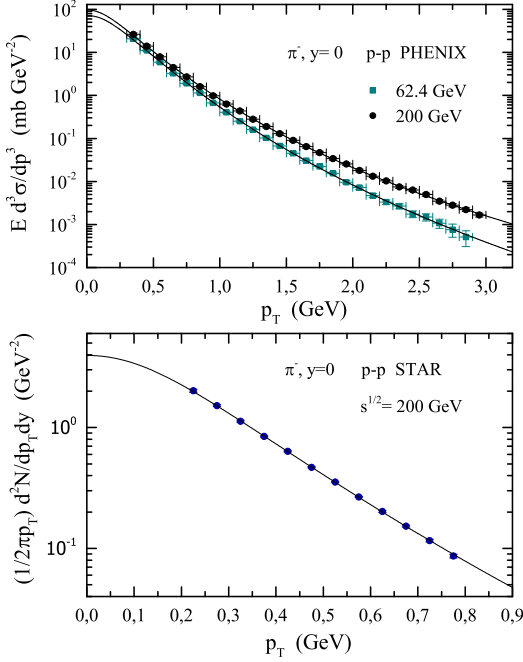


Fig. 2. (Color online) Transverse momentum distribution of negatively charged pions π^- produced in pp collisions as obtained by the PHENIX Collaboration [13,14] at $\sqrt{s} = 200$ and 62.4 GeV at mid-rapidity (upper panel) and by the STAR Collaboration [11,12] at $\sqrt{s} = 200$ GeV in the minimum bias (lower panel). The solid curves are the fits of the data to the Tsallis distribution (8) at rapidity $y = 0$.

differ from the exponential function. The values of the parameter q are greater than unity.

Figure 3 represents the transverse momentum distributions of the negatively charged pions π^- produced in pp collisions as obtained by the CMS Collaboration [18, 19] at $\sqrt{s} = 0.9, 2.76$ and 7 TeV in the rapidity interval $|y| < 1$ and by the ALICE Collaboration [16] at $\sqrt{s} = 0.9$ TeV in the rapidity interval $|y| < 0.5$. The symbols represent the experimental data. The solid curves are the fits of the experimental data to the Tsallis function (6); the values of the parameters of the Tsallis function (6) are given in Tab. 1. The experimental data of the CMS Collaboration for the transverse momentum distributions of the negatively charged pions are described very well by the power law function (6) with exception only of the lowest p_T data (see the upper panel of Fig. 3). The experimental data of the ALICE Collaboration at $\sqrt{s} = 0.9$ TeV for π^- pions are described very well by the function (6) in all p_T region (see the lower panel of Fig. 3). Thus the experimental transverse momentum distributions of π^- pions measured by the ALICE and CMS Collaborations cannot be described by the exponential function.

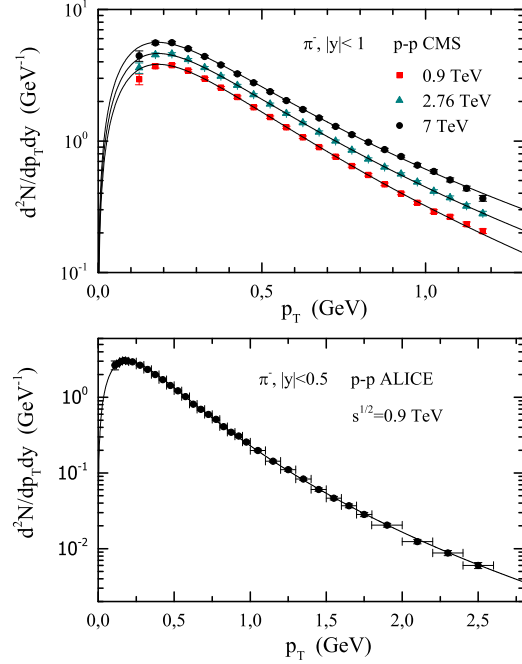


Fig. 3. (Color online) Transverse momentum distribution of negatively charged pions π^- produced in pp collisions as obtained by the CMS Collaboration [18,19,20] at $\sqrt{s} = 0.9, 2.76$ and 7 TeV in the rapidity interval $|y| < 1$ (upper panel) and by the ALICE Collaboration [16] at $\sqrt{s} = 0.9$ TeV in the rapidity interval $|y| < 0.5$ (lower panel). The solid curves are the fits of the data to the Tsallis distribution (6).

The energy dependence of the parameters of the Tsallis distribution for the negatively charged pions π^- produced in pp collisions is shown in Fig. 4. The parameters of π^- pion distributions are compared with the parameters of the charged hadron distributions given in Ref. [30]. Solid points are results of the fit for the negatively charged pions π^- . Open points are results of the fit for the charged hadron distributions produced in pp and $p\bar{p}$ collisions as obtained by the ATLAS, ALICE and UA1 Collaborations, respectively [30]. Open stars are results of the fit at $y = 0$ for the data of NA61/SHINE Collaboration. The values of the parameters are given in the Table 1 and 2.

It is clearly seen that the transverse momentum distribution of π^- pions has a power law form and increasingly deviates from the exponential function with collision energy (the parameter q is not equal to unity and increases with \sqrt{s}). Within the range of beam energies considered here the dependence of q on \sqrt{s} is linear on a logarithmic scale. To show explicitly this dependence we parametrize the parameter q for π^- pions by the function of the form

$$q = 1 + \ln \left(\frac{\sqrt{s}}{\sqrt{s_0}} \right)^{a_0}, \quad (9)$$

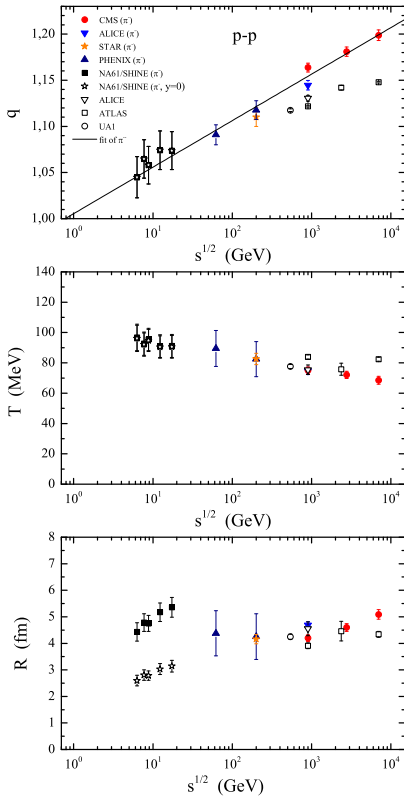


Fig. 4. (Color online) Energy dependence of the temperature T , radius R and the parameter q of the Tsallis distribution. Solid points are results of the fit for the negatively charged pions π^- produced in pp collisions as obtained by the NA61/SHINE [37], PHENIX [13,14], STAR [11,12], ALICE [16] and CMS [18,19] Collaborations. Open stars are results of the fit at $y = 0$ for the data of NA61/SHINE. Open squares, triangles and circles are results of the fit for the charged hadron yields produced in pp and $p\bar{p}$ collisions as obtained by the ATLAS, ALICE and UA1 Collaborations, respectively (taken from Ref. [30]). Data for the parameter q for π^- were fitted by Eq. (9).

where $a_0 = 0.0219 \pm 0.0014$ and $\sqrt{s_0} = 0.7805 \pm 0.3673$ GeV. Eventually this rise will come to a halt and reach the asymptotic limit $4/3$ discussed earlier in this paper. For the suggested linear parametrization this happens at extremely high energies, being even higher than the highest energies of protons in cosmic rays.

At NA61/SHINE energies the parameter q for π^- pions is close to unity. Let us stress that the use of the pion data instead of data for charged hadrons first used in [30] and explored in [31] allows us to obtain a much better fit than in previous analyses.

With increasing beam energy, as attained in PHENIX, STAR, ALICE and CMS, the parameter q for π^- pions clearly increases and becomes significantly different from unity. Note that the values of the parameter q for π^- pions measured by the CMS Collaboration differ from the values

of the parameter q of charged hadrons obtained by the ALICE and ATLAS Collaborations.

As seen in the top panel of Fig. 4, the temperature $T \sim 100$ MeV of π^- pions slowly decreases with the energy of the collision. The greater the deviation of the distribution function from the exponential function, the smaller the temperature is. The values of the temperature T for π^- pions measured at PHENIX, STAR and ALICE energies are significantly smaller than the values of the temperature T of the negatively charged pions obtained at NA61/SHINE energies. Note that the values of the temperature T of the charged hadrons measured by the ATLAS Collaboration given in Ref. [30] differ from the values of the temperature T of π^- pions of the CMS Collaboration obtained by the Tsallis distribution (6). For comparison, using the standard blast-wave description, as used e.g. in [41] leads to a similar value kinetic freeze-out temperature of $T_{kin} = 95 \pm 10$ MeV for an average transverse expansion velocity of $\langle \beta_T \rangle = 0.65 \pm 0.02$ albeit for heavy-ion collisions.

One can also attribute such energy behaviour to the interplay of longitudinal and transverse degrees of freedom. The temperature in the longitudinal p_L space is of the order of tens of GeV and depends on the available energy and multiplicity of secondaries [9]. Thus, a slight decrease in temperature with energy may be explained by the fact that most part of the energy of the system flows in the longitudinal direction. This may be considered as a sort of implementation of suggestion [40], that "higher collision energies do not increase the transverse momenta temperature but increase instead the number of involved bosons that are produced (like water boiling at higher flux of energy, where only the rate of vapor production is increased, but not the temperature)".

As seen in the middle panel of Fig. 4, the radius R for π^- pions is only mildly dependent on the energy of the collision. The values of the radius R of the system for π^- pions differ essentially from the geometrical sizes of the compound system of two protons. However, the values of the radius R for π^- pions are consistent with the values of the radius R for the charged hadrons given in Ref. [30]. It is interesting that maximal value of radius appears in the same energy region as famous "horn" in the kaons relative multiplicity.

3 Discussion and conclusions

The experimental data on the transverse momentum distribution of the negatively charged pions produced in pp collisions at different energies were fitted to the Maxwell-Boltzmann distribution of the Tsallis statistics at zero chemical potential. We have found the energy dependence of the parameters T , R and q of the Tsallis distribution of the negatively charged pions in the energy range $6.6 < \sqrt{s} < 7000$ GeV. We have revealed that the deviation of the transverse momentum distribution of negatively charged pions from the exponential function toward the power law distribution increases with energy of pp collisions. We have found that the parameter q increases with

Collaboration	\sqrt{s} , GeV	T , MeV	R , fm	q	χ^2/ndf
NA61/SHINE	6.3	96.76 \pm 8.69	4.431 \pm 0.344	1.0449 \pm 0.0223	2.704/15
NA61/SHINE	7.7	92.68 \pm 7.67	4.782 \pm 0.334	1.0647 \pm 0.0208	1.140/15
NA61/SHINE	8.8	95.39 \pm 7.33	4.749 \pm 0.301	1.0580 \pm 0.0204	0.989/15
NA61/SHINE	12.3	91.03 \pm 7.43	5.172 \pm 0.350	1.0741 \pm 0.0209	0.891/15
NA61/SHINE	17.3	91.17 \pm 7.56	5.358 \pm 0.375	1.0736 \pm 0.0205	0.459/15
PHENIX	62.4	89.52 \pm 11.83	4.379 \pm 0.853	1.0909 \pm 0.0108	0.938/23
PHENIX	200.0	82.50 \pm 11.56	4.255 \pm 0.861	1.1177 \pm 0.0101	0.758/24
STAR	200.0	82.57 \pm 3.74	4.159 \pm 0.173	1.1100 \pm 0.0100	2.738/9
ALICE	900.0	74.69 \pm 2.37	4.686 \pm 0.125	1.1446 \pm 0.0051	2.183/30
CMS	900.0	75.02 \pm 2.30	4.198 \pm 0.124	1.1637 \pm 0.0048	11.080/19
CMS	2760.0	72.10 \pm 2.38	4.597 \pm 0.144	1.1809 \pm 0.0051	7.425/19
CMS	7000.0	68.53 \pm 2.62	5.090 \pm 0.182	1.1987 \pm 0.0057	11.500/19

Table 1. Parameters of the Tsallis fit for π^- mesons produced in pp collisions at different energies.

\sqrt{s} , GeV	T , MeV	R , fm	q	χ^2/ndf
6.3	96.12 \pm 8.64	2.597 \pm 0.201	1.0449 \pm 0.0223	2.704/15
7.7	92.05 \pm 7.62	2.803 \pm 0.196	1.0648 \pm 0.0208	1.140/15
8.8	94.76 \pm 7.28	2.784 \pm 0.177	1.0580 \pm 0.0204	0.989/15
12.3	90.44 \pm 7.39	3.031 \pm 0.205	1.0741 \pm 0.0209	0.892/15
17.3	90.57 \pm 7.52	3.140 \pm 0.220	1.0737 \pm 0.0205	0.459/15

Table 2. Parameters of the Tsallis fit at $y = 0$ for π^- pions measured at NA61/SHINE energies.

beam energy while the temperature T slowly decreases. The radius R in pp collisions is a constant independent on the energy. At small values of energy of collision, where the transverse momentum distribution of negatively charged pions is close to the exponential function, the temperature is largest. It is interesting, that parameter q turns to 1 at low (unphysical) energy surprisingly close to ρ -meson mass, which is the natural hadronic scale.

Acknowledgments: We are indebted to G.I. Lykasov and A.S. Sorin for stimulating discussions. This work was supported in part by the joint research project and grant of JINR and IFIN-HH (protocol N 4543), by the Program of South Africa-JINR collaboration, and by RFBR (grant 14-01-00647).

References

1. C. Tsallis, J. Stat. Phys. **52** (1988) 479-487.
2. I. Bediaga, E.M.F. Curado and J.M. de Miranda, Phys. A **286** (2000) 156.
3. C. Beck, Phys. A **286** (2000) 164.
4. G. Wilk, Z. Włodarczyk, Phys. Rev. Lett. **84** (2000) 2770.
5. D.B. Walton, J. Rafelski, Phys. Rev. Lett. **84** (2000) 31.
6. W.M. Alberico, A. Lavagno, P. Quarati, Nucl. Phys. A **680** (2000) 94.
7. J. Zimányi, P. Lévai, T.S. Biró, J. Phys. G: Nucl. Part. Phys. **31** (2005) 711.
8. T.A. Trainor, Int. J. Mod. Phys. E **17** (2008) 1499.
9. G. Wilk, Z. Włodarczyk, Eur. Phys. J. A **40** (2009) 299.
10. T.S. Biró, K. Ürmösy, J. Phys. G: Nucl. Part. Phys. **36** (2009) 064044.
11. B. I. Abelev et al. (STAR collaboration), Phys. Rev. C **75**, 064901 (2007).
12. B.I. Abelev et al. (STAR Collaboration), Phys. Rev. C **79**, 034909 (2009)
13. A. Adare et al. (PHENIX collaboration), Phys. Rev. D **83**, 052004, (2011);
14. A. Adare et al. (PHENIX collaboration), Phys. Rev. C **83**, 064903 (2011).
15. K. Aamodt, et al. (ALICE collaboration), Phys. Lett. B **693**, 53 (2010).
16. K. Aamodt et al. (ALICE Collaboration), Eur. Phys. J. C **71**, 1655 (2011)
17. K. Aamodt, et al. (ALICE collaboration), Eur. Phys. J. C **73**, 2662 (2013).
18. V. Khachatryan, et al. (CMS collaboration), JHEP **02**, 041 (2010);
19. V. Khachatryan, et al. (CMS collaboration), Phys. Rev. Lett. **105**, 022002 (2010).
20. S. Chatrchyan et al. (CMS Collaboration), Eur. Phys. J. C **72**, 2164 (2012)
21. G. Aad, et al. (ATLAS collaboration), New J. Phys. **13**, 053033 (2011).
22. G. Biró, G.G. Barnaföldi, T.S. Biró, K. Ürmösy, arXiv:1608.0143.
23. H. Zheng, L. Zhu, Adv. High Energy Physics, 2016 (2016) 9632126.
24. Y-Q Gao, F-H Liu, Indian J. Phys. **90** (2016) 319.
25. H. Zheng, L. Zhu, Adv. High Energy Physics, 2015 (2015).
26. H. Zheng, L. Zhu, A. Bonasera, Phys. Rev. D **92** (2015) 074009.
27. G. Wilk, Z. Włodarczyk, Entropy **17** (2015) 384.
28. L. Marques, J. Cleymans, A. Deppman, Phys. Rev. D **91** (2015) 054025.
29. K. Ürmösy, G. G. Barnaföldi, S. Harangozó, T. S. Biró and Z. Xu, arXiv:1501.02352.
30. J. Cleymans, G. I. Lykasov, A. S. Parvan, A. S. Sorin, O. V. Teryaev, D. Worku, Phys. Lett. B **723** 351, 2013.
31. M. Rybczynski, Z. Włodarczyk, Eur. Phys. J. C **74**, 2785 (2014).
32. C.Y. Wong, G. Wilk Phys. Rev. D **87** (2013) 114007.

- 33. C.Y. Wong, G. Wilk, Acta Phys. Polonica **B 43** (2012) 2047.
- 34. C. Y. Wong, G. Wilk, L. J. L. Cirto, C. Tsallis, Phys. Rev. **D 91** (2015) 114027.
- 35. M.D. Azmi and J. Cleymans, Eur. Phys. J. **C 75** (2015) 430.
- 36. M. D. Azmi, J. Cleymans, J. Phys. **G 41**, 065001, 2014.
- 37. N. Abgrall et al. (NA61/SHINE Collaboration), Eur. Phys. J. **C 74**, 2794 (2014)
- 38. A.S. Parvan, PoS (Baldin ISHEPP XXII), 077 (2015)
- 39. F. Büyükkiliç, D. Demirhan, A. Güleç, Phys. Lett. A **197**, 209 (1995)
- 40. C. Tsallis, Chaos, Solitons & Fractals 13, 3 (2002) 371.
- 41. B. Abelev et al. (ALICE Collaboration) Phys. Rev. Lett. **109**, 252302 (2012).